A Strong Deviation from Vegard's Rule: X-Ray Powder Investigations of the Three Quasi-Binary Phase Systems BiOX–BiOY (X, Y = Cl, Br, I)

Egbert Keller and Volker Krämer

Kristallographisches Institut der Universität Freiburg, Hermann-Herder-Str. 5, D-79104 Freiburg

Reprint requests to Dr. E. Keller. Fax: +49761/203-6434. E-mail: egbert.keller@krist.uni-freiburg.de

Z. Naturforsch. **60b,** 1255 – 1263 (2005); received July 21, 2005

The three quasi-binary phase systems BiOX–BiOY (X, Y = Cl, Br, I) have been investigated by X-ray powder methods. No quaternary phases were found in the three systems. BiOCl–BiOBr and BiOBr–BiOI form systems of unlimited mutual solubility. BiOCl–BiOI is a system of limited solubility at the iodine-rich side. In the BiOBr–BiOI system a strong deviation from Vegard's rule is observed with respect to one of the lattice parameters. A few methods to quantify such a deviation are briefly discussed and a possible explanation for the strong deviation in the BiOBr–BiOI system is proposed. Error calculations have been performed to estimate uncertainties in the concentration parameter *x* of the investigated mixtures. The crystal structure of BiOI has been re-determined by single crystal structure analysis.

Key words: Bismuth Oxide Halides, Vegard's Law, X-Ray Powder Diffraction

Introduction

The simple bismuth oxide halides BiOX (X = Cl, Br, I) were already discovered in the 19th century [1]. Their structures were originally determined by Sillén in 1941 from powder diffraction data [2a], single crystal structure analyses were performed for BiOCl [2b] and BiOBr [2c] about half a century later. The three compounds are isotypic and crystallize in space group $P4/nmm$ (PbFCl structure type). The atomic arrangement consists of tetragonal $[Bi_2O_2]$ layers which are "sandwiched" by two halogen layers (Fig. 1). Vicinal $Bi_2O_2X_2$ layers interact mainly *via* Van-der-Waals forces. From BiOCl to BiOI the lattice parameter *a* grows by only 0.1 Å (from 3.89 to 3.98 Å) while *c* increases by 1.8 Å (from 7.35 to 9.13 Å).

Despite the fact that the BiOX compounds have been known for more than a century no investigations of reactions between them seem to have been performed up to now except for some commercially motivated work with the aim to design new pigments [3]. In the work described below we have investigated the three quasi-binary phase systems BiOCl–BiOBr, BiOCl–BiOI, and BiOBr–BiOI by means of X-ray powder methods. The initial aim of this work was to search for quaternary phases of formula $(BiO)_{n+m}X_nY_m$. Though the BiOX compounds are isotypic (meaning that they are no primary candidates for the formation of new phases) steric considerations made us believe that such quaternary compounds might exist.

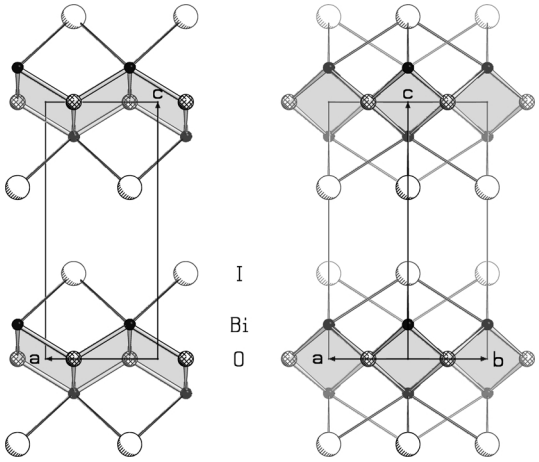

Fig. 1. The structure of BiOI as seen from [0 1 0] (left) and from [1 1 0] (right). Shaded areas denote $[Bi_2O_2]$ layers.

Furthermore we present the results of the still-to-be-done single crystal structure re-determination of BiOI.

Results and Discussion

The single crystal structure of BiOI confirms the results (basing on powder data) by Sillén [2a] the largest positional shift being 0.016 Å for Bi. The structure is

Table 1. Crystal data and structure refinement for BiOI.

Empirical formula	Bi I O
Formula weight	351.88
Temperature	293(2) K
Wavelength	0.71073 Å
Crystal system, space group	tetragonal, $P4/nmm$
Unit cell dimensions [Å]	$a = 3.995(2)$, $b = 3.995(2)$, $c = 9.151(5)$
Volume	146.05(13) Å^3
Z, Calculated density	2, 8.002 g/cm^3
Absorption coefficient	70.555 mm^{-1}
F_{000}	288
Crystal size	$0.300 \times 0.175 \times 0.003$ mm
θ Range for data collection	2.22 to 28.18°
Limiting indices	$-5 \le h \le 4$, $-2 \le k \le 5$, $-11 \le l \le 11$
Reflections collected / unique	871 / 134 [$R_{int} = 0.1013$]
Completeness to $\theta = 28.18°$	95.7%
Absorption correction	Numerical integration
Max. and min. transmission	0.7883 and 0.0314
Refinement method	Full-matrix least-squares on F^2
Data / restraints / parameters	134 / 0 / 10
Goodness-of-fit on F^2	1.073
Final R indices [$I > 2\sigma(I)$]	$R_1 = 0.0184$, $wR_2 = 0.0416$
R Indices (all data)	$R_1 = 0.0184$, $wR_2 = 0.0416$
Extinction coefficient	0.0065(12)
Largest diff. peak and hole	2.137 and -1.145 eÅ^{-3}

Table 2. Atomic coordinates and displacement parameters for BiOI. The anisotropic displacement factor exponent takes the form: $-2\pi^2[h^2 a^{*2} U_{11} + \ldots + 2hk a^* b^* U_{12}]$; U_{eq} is defined as one third of the trace of the orthogonalized U_{ij} tensor. U_{ij} $(i \neq j) = 0$.

Atom	x	y	z	$U_{11} = U_{22}$	U_{33}	U_{eq}
Bi	1/4	1/4	0.1338(1)	0.0125(3)	0.0165(3)	0.0138(3)
I	1/4	1/4	0.6671(1)	0.0141(4)	0.0162(4)	0.0148(3)
O	1/4	3/4	0	0.011(2)	0.014(3)	0.012(2)

Table 3. Bond lengths [Å] for BiOI.

Bi-O	2.343(1)	Bi-I	3.362(1)

visualized in Fig. 1, crystal and refinement data, positional and displacement parameters of the atoms, and bond lengths are given in Tables 1 to 3*.

The results of our powder X-ray investigations of BiOX/BiOY mixtures indicate that actually no quaternary compounds are formed in the three BiOX–BiOY systems. In the two systems BiOCl–BiOBr and BiOBr–BiOI the end members form solid solutions over the whole composition range. In the system BiOCl–BiOI, BiOI can dissolve up to 26% BiOCl

*Further details of the crystal structure investigation are available from the Fachinformationszentrum Karlsruhe, D-76344 Eggenstein-Leopoldshafen (Germany), on quoting the depository number CSD-391354, the name of the author(s), and citation of the paper.

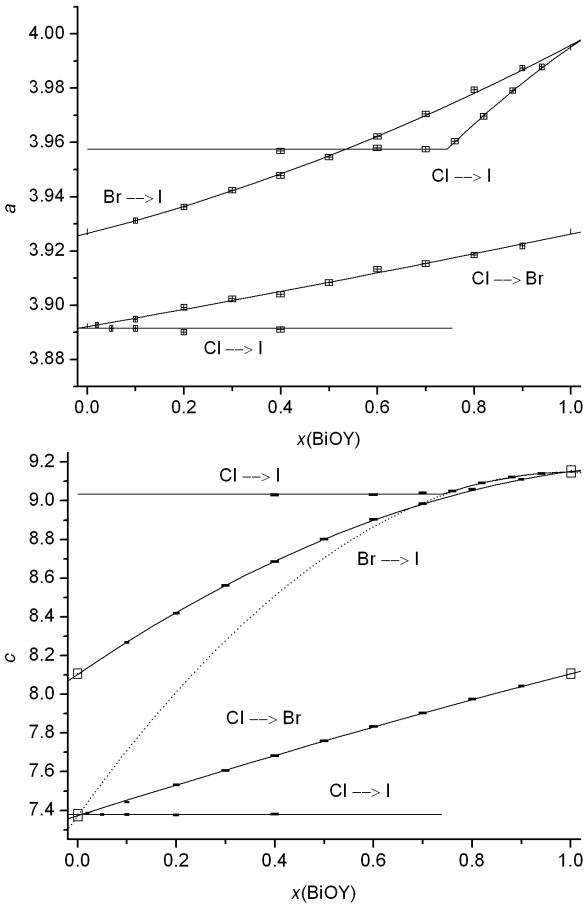

Fig. 2. $a(x)$ (top) and $c(x)$ (bottom) graphs for the three BiOX–BiOY systems. Rectangles ("bars") representing the data points generally visualize errors (uncertainties) in x and $a(c)$. The rectangles at $x = 0$ and 1 (bottom) simply indicate the positions of the respective data points (errors of which are too small to produce a visible data "bar").

but BiOCl can dissolve only very small amounts of BiOI, if any (0 – 2%). In binary metal alloys, unlimited solubility is usually only observed if the difference in the atomic radii of the components is not more than about 15% [4]. A similar rule exists also for the general case of solid solutions [5]. For BiOX–BiOY, the corresponding differences between the halogen ionic radii (Cl = 1.81, Br = 1.95, I = 2.20 Å [6]) are about 8% for Cl/Br and 12% for Br/I but 20% for Cl/I. Measured lattice parameters for the different mixtures are collected in Table 5 and visualized in Fig. 2 as functions of the concentration parameter $x = n_B/(n_A + n_B)$ where n_A, n_B are the molar quantities of end members A and B. Note that the shapes of the data "points" in Fig. 2 visualize uncertainties in x as well as in the lattice pa-

System	t	A [Å]	B_1 [Å]	B_2 [Å]	θ [Å]	$\Delta t_{0.5}$ [Å]
Cl–Br	*a*	3.892(1)	0.031(3)	0.003(3)	−0.003(2)	−0.000(1)
Br–I	*a*	3.926(1)	0.046(3)	0.024(4); (*3*)[a]	−0.023(3); (*2*)	−0.006(1)
Cl–I	*a*	3.77(2)	0.31(5)	−0.10(3)		
Cl–Br	*c*	7.369(3)	0.82(4); (*1*)	−0.08(4); (*1*)	0.08(3); (*1*)	0.021(7); (*2*)
Br–I	*c*	8.101(3)	1.74(7); (*1*)	−0.69(8); (*1*)	0.69(5); (*1*)	0.173(12); (*2*)
Cl–I	*c*	7.375(3)	3.56(5); (*2*)	−1.78(4); (*2*)	1.78(3); (*1*)	[0.446(8); (*4*)]
	c[b]	7.60(8)	3.0(2)	−1.5(1)	1.4(1)	[0.34(3)]

Table 4. Parameters quantifying the 2nd order functions in Fig. 2.

[a] Standard deviations printed in italics have been conventionally derived from least-squares fitting; [b] data point at $x = 0$ excluded.

rameter values (see section "Error Calculations"). With respect to the pure end members of the three systems, the lattice parameters for BiOBr and a_{BiOCl} agree well with those previously reported [2b,c] while those for BiOI [2a] and c_{BiOCl} [2b] are larger by 0.01 – 0.02 Å.

Quantifying deviations from Vegard's rule

Lattice-constant-versus-concentration data in solid solution systems of unlimited miscibility can in most cases be closely approximated by functions of 1st or 2nd order. If linearity (1st order function) is observed, the system is said to follow Vegard's rule [7]. In this case, the lattice parameter (named t in the following) varies with x according to

$$t(x) = t_{\mathrm{A}}(1-x) + t_{\mathrm{B}}x = t_{\mathrm{A}} + (t_{\mathrm{B}} - t_{\mathrm{A}})x = t_{\mathrm{V}}(x) \quad (1)$$

with t_{A}, t_{B} being the lattice parameters of end members A and B. In the case of 2nd order the deviations from Vegard's rule can be quantified by a so-called "bowing parameter" θ [8]:

$$\begin{aligned} t(x) &= t_{\mathrm{A}} + (t_{\mathrm{B}} - t_{\mathrm{A}})x + \theta(x - x^2) \\ &= t_{\mathrm{V}}(x) + \theta(x - x^2). \end{aligned} \quad (2)$$

V. Steinwehr has introduced a related parameter ϕ [9]. By comparison we find $\phi = \theta/(t_{\mathrm{A}} + t_{\mathrm{B}})$. Thus, ϕ is a relative bowing parameter with twice the average cell parameter $t_{\mathrm{V}(0.5)}$ as the reference value. Another quantity, which has been used to measure deviations from Vegard's rule is the difference between $t(x)$ and $t_{\mathrm{V}}(x)$ for $x = 0.5$ [8a, 10, 11], called $\Delta t_{0.5}$ in the following. If the function $t(x)$ is of 2nd order we can derive

$$\Delta t_{0.5} = t(0.5) - t_{\mathrm{V}}(0.5) = \theta(0.5 - 0.25) = \theta/4 \quad (3)$$

from eq. (2). If any other values Δt_x are known instead of $\Delta t_{0.5}$ and, again, if the function $t(x)$ is of 2nd order, θ can be approximated as an average value from Δt_x according to

$$\theta = \langle \Delta t_x/(x - x^2) \rangle. \quad (4)$$

Like θ, $\Delta t_{0.5}$ can in principle be replaced by a relative parameter with $(t_{\mathrm{A}} + t_{\mathrm{B}})$ or $(t_{\mathrm{A}} + t_{\mathrm{B}})/2$ as the reference value. This is, however, reasonable only if *all* parts of the structures in question are affected by changes in x. Furthermore, deviations from Vegard's law have also been set in relation to the lattice parameter difference $|t_{\mathrm{A}} - t_{\mathrm{B}}|$ [9, 19b]; as a consequence, small absolute deviations from linearity result in large parameter values if t_{A} and t_{B} are similar.

In the following, we will exclusively use the bowing parameter θ and its easier to understand quarter, $\Delta t_{0.5}$, as a measure of deviations from Vegard's rule. *In praxi*, θ can be determined by fitting a function of 2nd order ($f(x) = A + B_1 x + B_2 x^2$) to the data. This may, of course, be done as an approximation even in cases where functions of higher order seem more appropriate to represent the data. From eq. (2) we get

$$t(x) = t_{\mathrm{A}} + (t_{\mathrm{B}} - t_{\mathrm{A}} + \theta)x - \theta x^2. \quad (5)$$

By comparison and averaging we obtain

$$\begin{aligned} &\theta = [(B_1 - t_{\mathrm{B}} + t_{\mathrm{A}}) - B_2]/2 \text{ with} \\ &\mathrm{d}\theta = \frac{1}{2}(\mathrm{d}{B_1}^2 + \mathrm{d}{B_2}^2 + \mathrm{d}{t_{\mathrm{B}}}^2 + \mathrm{d}{t_{\mathrm{A}}}^2)^{1/2}. \end{aligned} \quad (6)$$

Application to BiOX–BiOY systems

In Fig. 2, to most of the different groups of data [*a vs. x*] or [*c vs. x*] functions of 2nd order have been fitted. In the case of $c(x)$ (BiOCl–BiOI system) *two* functions have been fitted to the data with $x < 0.74 < 1$: for one function (solid line) no additional data have been accounted for, for the other function (dotted line) the point at $x = 0$ was included. Data which are obviously independent of x have been fitted by straight lines with a fixed slope of 0. Taking the possible errors in data point positions into account (see section "Error Calculations") it becomes clear that no functions of order > 2 are necessary to describe the various $t(x)$ functions in the BiOX–BiOY systems. The different parameters of the 2nd order functions and the parameters θ and $\Delta t_{0.5}$

quantifying the deviation of $t(x)$ from linearity in our BiOX–BiOY (= $BiOX_{1-x}Y_x$) systems are collected in Table 4.

As can be seen from Fig. 2 and Table 4, $a(x)$ shows no significant deviation from Vegard's rule for $BiOCl_{1-x}Br_x$ and a slight, but significant, negative deviation for $BiOBr_{1-x}I_x$. For $BiOCl_{1-x}I_x$ ($x < 0.74 < 1$) we get a strongly negative deviation with a slightly negative B_2 value such that there is no chance to connect the curve with the data point at $x = 0$ without using a function of order > 2. A $t(x)$ curve with similar (even more pronounced) features has been obtained from density-functional theory calculations for a hard-sphere model of a binary solid solution. From a series of curves corresponding to different radius differences the curve in question is the one calculated for the largest difference (15%) (but note that different points on this calculated curve correspond to different temperatures). The corresponding simulated phase diagram corresponds to a eutectic system with limited solubility [12].

$c(x)$ shows a slight, just significant positive deviation in $BiOCl_{1-x}Br_x$ and a clearly significant positive deviation with $\Delta t_{0.5} = 0.17(1)$ Å in $BiOBr_{1-x}I_x$. For $BiOCl_{1-x}I_x$ ($x < 0.74 < 1$) we get a severe deviation of "$\Delta t_{0.5}$" = 0.45(1) Å (or 0.34(3) Å if the data point at $x = 0$ is excluded from the fitting). Quotation marks are used here to indicate, that these $\Delta t_{0.5}$ values are "virtual", as the phase doesn't exist for $x = 0.5$. It should be noted that for both versions of the $c(x)$ function (dotted line and solid line in Fig. 2b) the slope at $x = 1$ is zero. On the (unchecked) hypothesis that the replacement of a smaller anion (Cl) by a larger one (I) should never lead to a *de*crease of the lattice parameters, this would be the *minimal* slope generally possible.

When looking for $\Delta t_{0.5}$ values derived from data published for other systems with *unlimited* solubility (a search certainly far from completeness), we found values of magnitudes less than 0.03 Å for III–V semiconductors [8b, 13], binary compounds with zincblende structure [11], and simple halides (AX) including mixed-anion systems like $KBr_{1-x}I_x$ [11, 14]; the majority of alloys obeys these limits as well, most others yield values less than 0.075 Å [9, 15], a rather extreme exception being $c(x)$ in Cd–Mg at a temperature of 310 °C with $\Delta t_{0.5} = -0.31$ Å [15]. In most other inorganic systems with unlimited solubility, $|\Delta t_{0.5}|$ seems to be below 0.06 Å. Deviations leading to $|\Delta t_{0.5}|$ values in the range 0.03 to 0.05 Å are occasionally addressed as "large" or "(very) strong" [16] thus encouraging us to classify the deviation in our $BiOBr_{1-x}I_x$ system with $\Delta t_{0.5} = 0.17$ Å "strong" as well. Naturally, systems with *limited* solubility (where generally |"$\Delta t_{0.5}$"| values much larger than 0.10 Å can occur [17]) are not part of the competition here. Our $BiOCl_{1-x}I_x$ system with "$\Delta t_{0.5}$" = 0.45(1) Å (see above) provides a relevant example.

It should be noted that a similar "$\Delta t_{0.5}$" value of 0.43(4) Å can be deduced from data published for the related $SrFCl_{1-x}I_x$ system which also crystallizes with the PbFCl structure [18]. In this system, the solubility is also very restricted (to $\approx 0.9 < x < 1$). In contrast to this similarity, the data published for $SrFBr_{1-x}I_x$ [18] are "incompatible" with those for $BiOBr_{1-x}I_x$ in as much as there is a miscibility gap for $\approx 0.2 < x < \approx 0.6$ with *no* deviation from Vegard's law for $x > 0.6$ and a severe *negative* deviation for $x < 0.2$. We found no other data for mixed Br/I systems with a PbFCl structure.

Attempt to explain the observed strong deviation from Vegard's rule

Returning to systems with *unlimited* solubility we found $\Delta t_{0.5}$ values > 0.1 Å (as in $BiOBr_{1-x}I_x$) also for $c(x)$ in $Hf(Se_{1-x}Te_x)_2$ ($\Delta t_{0.5} = 0.12$ Å), $Hf(S_{1-x}Te_x)_2$ (0.22 Å) [10], and for the intercalates Li_xC_6 (≈ 0.11 Å) and Li_xTiS_2 (≈ 0.20 Å) [19a]. The end members of these systems (crystals of which all belong to the hexagonal crystal *family*) exhibit structures similar to BiOX: they consist of electrically neutral layers interacting mainly *via* Van der Waals forces (with respect to the Li compounds this is, of course, true only for the end member with $x = 0$). Another feature common with $BiOBr_{1-x}I_x$ is that Δa values are much smaller than Δc values and that $\Delta t_{0.5}$ for $a(x)$ is around zero.

For $Hf(Ch_{1-x}Ch'_x)_2$ and other $M(Ch_{1-x}Ch'_x)_2$ systems (Ch = chalcogenide) the positive deviations of $c(x)$ from Vegard's law have been explained as follows [10]: It is assumed that the M–Ch bond length varies linearily with x which necessarily leads to repulsions between vicinal anions of the larger chalcogen, the two members of an anion pair belonging to the two different anion layers of one and the same sandwich. Relaxation of the MCh_2 sandwiches in order to reduce these repulsions are then supposed to be mainly responsible for the observed deviations from linearity. At least for our BiOX compounds we would prefer another explanation: First, as has been shown by EXAFS measurements [11], M–X and M–Y bonds of different

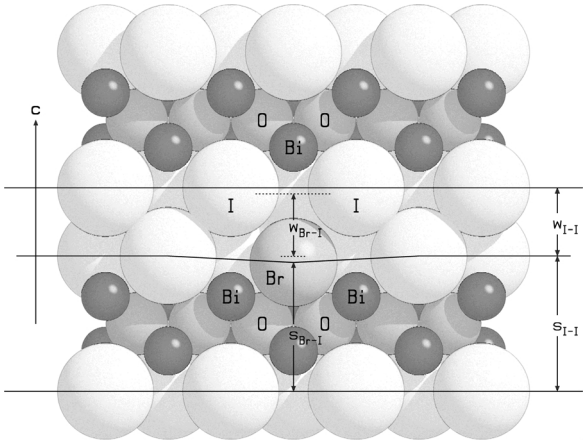

Fig. 3. A [1 1 0] view of the BiOI structure with one I atom replaced by Br. The Br atom has been moved downwards from its original position (see text), the rest of the structure has been left unchanged.

lengths coexist in a mixed crystal $M_p(X_{1-x}Y_x)_q$. Furthermore, we assume that the strong bowing of $c(x)$ is mainly due to the weakness of anion-anion interactions across the interface between two vicinal sandwiches.

In Fig. 3, an I atom in the structure of BiOI has been replaced by a (smaller) Br atom. A section of the structure (of thickness c) has been divided into two parts: The "sandwich" of thickness $s_{\text{I-I}}$ and the anion-anion interface of thickness $w_{\text{I-I}}$. Comparatively strong bonding forces have made the Br atom move from the original I position towards the Bi atoms it is bonded to such that a Bi-Br distance (approximately) equal to the one in BiOBr has been adopted. The thickness $s_{\text{I-I}}$ of the lower sandwich at the Br position will therefore be $s_{\text{Br-I}} = (s_{\text{I-I}} + s_{\text{Br-Br}})/2$, $s_{\text{Br-Br}}$ being the sandwich thickness in pure BiOBr. The *average* thickness of the lower sandwich, s(av), will then be as demanded by Vegard's rule. To have the thickness w(av) of the I-I interface (and thus the *whole* structure) also follow this rule, $w_{\text{I-I}}$ (or, better, the distance $d = c - s_{\text{Br-I}}$) is required to shrink to $w_{\text{Br-I}}$ at the Br position, *i.e.*, the centers of the atoms labelled Br and I in Fig. 3 would each have to move parallel $-\boldsymbol{c}$ (I) or $+\boldsymbol{c}$ (Br) by about 0.26 Å (*i.e.*, to the broken lines), drawing along the atoms to which they are bonded (labelled "Bi" in Fig. 3) and those to which the latter are bonded (*e.g.* the atoms labelled "O" in Fig. 3). However, due to the *one-sidedness* of the halogen coordination polyhedra this movement is induced by nothing else but the weak Van der Waals attraction between Br and I, and it is thwarted by strong I-I and I-O repulsions and by the rigidity of the $[Bi_2O_2]^{2+}$ layers. The balance point between attraction and repulsion is therefore assumedly reached at X positions "far" outside the region defined by the two broken lines in Fig. 3, thus making the large positive deviation from Vegard's law ($\Delta t_{0.5} = 0.17$ Å) understandable. For systems with all coordination polyhedra *closed* like $KBr_{1-x}I_x$ [14a] or the arbitrarily selected $Ba_2Pb_4F_{10}(Br_{1-x}I_xF)_2$ containing *single* (Br,I) layers [20], much smaller $\Delta t_{0.5}$ values (< 0.02 Å) are found.

It should be noted that the model of Fig. 3 has been designed under the assumption that $\varepsilon = 1$ [11], *i.e.*, that bond lengths in mixed crystals are (or tend to be) just as they are in the end components, but the arguments would be the same if ε was reduced to, say, 0.6 (corresponding to a partial convergence of M-X and M-Y bond lengths like in mixed alkali halides [11]).

At first sight, the power of persuasion of the explanation proposed above (as, by the way, of any other explanation based on X, Y size differences!) is somewhat reduced by the observation that the deviation of $c(x)$ from linearity is much slighter in the case of $BiOCl_{1-x}Br_x$. From radius differences Δr (0.15 *vs.* 0.24 Å or 8 *vs.* 12%, see above) one would initially expect an effect of at least half the magnitude of that of $BiOBr_{1-x}I_x$. Instead, only about one eighth is observed. The values found for the $Hf(Ch_{1-x}Ch'_x)_2$ systems mentioned above and containing also anion-anion interface layers seem to be much more consistent: $Hf(S_{1-x}Se_x)_2$ ($\Delta r = 0.14$, $\Delta t_{0.5} = 0.06$ Å); $Hf(Se_{1-x}Te_x)_2$ ($\Delta r = 0.23$, $\Delta t_{0.5} = 0.12$ Å); $Hf(S_{1-x}Te_x)_2$ ($\Delta r = 0.37$, $\Delta t_{0.5} = 0.22$ Å) [10]. However, we feel free to include also the "$\Delta t_{0.5}$" value for $BiOCl_{1-x}I_x$, which is a virtual value but nevertheless quantifies the behaviour of this system in the range ($0.74 < x < 1$). If now $\Delta t_{0.5}$ is plotted against Δr we obtain a linear relationship for our three BiOX–BiOY systems which is equally well defined as the one for the three $Hf(Ch_{1-x}Ch'_x)_2$ systems. This is shown in Fig. 4 where also the data for three $Ti(Ch_{1-x}Ch'_x)_2$ systems [10] have been plotted. The observation that the straight lines in Fig. 4 intersect the (dotted) line $\Delta t_{0.5} = 0$ at positive Δr values suggests that there might be an additional effect at work which would lead to negative deviations from Vegard's law if it was not overcompensated (for larger Δr values) by effects caused by the anion size difference. The comparatively large slope of the straight line representing the $BiOX_{1-x}Y_x$ systems can be related to the increased rigidity [19b] of the $[Bi_2O_2]$ layers as compared to

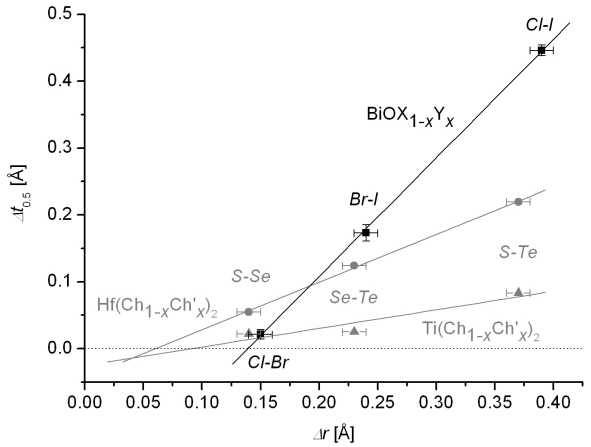

Fig. 4. Plot of the deviation parameter $\Delta t_{0.5}$ *vs.* the anion radius difference Δr for three groups of solid solutions. To the Δr values an estimated error of 0.01 Å has been assigned.

those of the M layers of the mixed chalcogenide systems.

Finally, we will briefly discuss the above mentioned intercalates Li_xC_6 ($\Delta t_{0.5} \approx 0.11$ Å) and Li_xTiS_2 ($\approx$ 0.20 Å), which are different cases, for once because the approximation of the $c(x)$ curves by functions of 2nd order is only very coarse [19]. Furthermore, instead of two anions of different sizes, voids of partial occupancy are present. Nevertheless we can calculate a formal approximate "Δr" value for Li_xTiS_2 from the S-S distances in TiS_2 (3.48 Å [21]) and in $LiTiS_2$ (3.81 Å [22]) which can be seen as a difference between the "void radius" and the Li radius. The corresponding value of 0.16 Å seems rather low with respect to the large $\Delta t_{0.5}$ value. On the other hand, intercalated Li atoms are oxidized to Li^{+1} and their electrons are partially delocalized within the TiS_2 layers [23]. One might therefore assume that the weak attraction between interface S layers (at positions where the voids are empty) is even more reduced by increased electrostatic S-S repulsion. Furthermore, the hardness of Li^+ is certainly higher than that of, *e.g.*, Br^- or Se^{2-}, meaning that Li^+ will presumably offer more resistance against attraction of the two interface layers (at vicinal positions with empty voids) than the latter (at vicinal positions with a smaller anion).

Experimental Section

Chemical analyses have been performed by AAS (Bi) and by argentometry (Cl,Br).

BiOCl: Commercial BiOCl (Merck, purity not specified) was used for the experiments. BiOCl (260.4): calcd. Bi 80.24, Cl 13.61; found Bi 79.24, Cl 13.40.

BiOBr was synthesized by heating a mixture of 1.470 g (3.15 mmol) Bi_2O_3 (Merck, 99%) and 1.440 g (3.21 mmol) $BiBr_3$ (Heraeus, 99%) at 500 °C in an evacuated quartz ampoule for 2 days. Excess $BiBr_3$ was then separated from the product by sublimation from 400 to 300 °C. The reaction product was mortared and put into another evacuated quartz ampoule. By sublimaton from 400 to 300 °C residual $BiBr_3$ was removed. A powder diffractogram of the product showed the (only) crystalline phase in it to be BiOBr. BiOBr (304.9): calcd. Bi 68.54, Br 26.21; found Bi 68.03, Br 25.50.

BiOI was synthesized by heating a mixture of 0.932 g (2 mmol) Bi_2O_3 (Merck, 99%) and 1.240 g (2.1 mmol) BiI_3 (Aldrich, 99%) at 550 °C in an evacuated quartz ampoule for 2 days. Excess BiI_3 was then separated from the product by sublimation from 300 to 200 °C. The product was mortared and put into another evacuated quartz ampoule. By sublimaton from 300 to 200 °C residual BiI_3 was removed. A powder diffractogram of the product showed the (only) crystalline phase in it to be BiOI. BiOI (351.9): calcd. Bi 59.39; found Bi 59.89. I was not determined as BiOI can only be dissolved in HNO_3 which oxidizes I^- to I_2 and $IO_3{}^-$.

Single crystals of BiOI: About 0.05 g BiOI powder was sealed in an evacuated quartz ampoule (length: 7 cm, internal diameter 0.5 cm, pressure $2 \cdot 10^{-6}$ Torr). The ampoule was placed in a half-shell two-zone furnace with the two half-shells separated by a sheet of fiberfrax (with a small hole) such that one half of the ampoule was positioned in the lower shell and the other half in the upper shell. The lower shell was heated to 725 °C while the upper shell was heated to 700 °C. After two days single crystals had grown in the upper part of the ampoule, some of which were black and bulky, while most others were very thin bright red platelets.

Structure re-determination of BiOI: One of the red platelets described above of size $0.30 \times 0.175 \times 0.003$ mm was investigated on a Bruker AXS SMART diffractometer with a CCD detector. After performing a numerical absorption correction the known structure was refined to $R1 = 0.0184$ [24]. For the final calculations the cell parameters obtained by the single crystal diffractometer ($a = 3.9739(5)$, $c = 9.115(1)$ Å) were replaced by those determined by powder diffraction (see below). The large differences of 0.02 Å in a and 0.04 Å in c are probably due to the extreme platelet shape of the crystal and the high absorption coefficient. To check this, a number of other single crystals (red platelets) grown in the same ampoule were mortared. A diffractogram of the powder obtained this way corresponded to lattice parameters which were identical (within 1.5 standard deviations) to those given in Table 5 for pure BiOI.

Mixtures of BiOX and BiOY, each mixture amounting to 100 ± 5 mg, were formed by mixing weighed amounts of BiOX and BiOY in a mortar. The mixtures were heated in

x	dx	a	c	x	dx	a	c
$BiOCl_{1-x}Br_x$				0.700	0.0074	3.9705(3)	8.984(1)
0.000	0.0000	**3.892(2)**[a]	**7.375(2)**	0.800	0.0065	3.9794(3)	9.059(1)
0.100	0.0045	3.8948(4)	7.443(3)	0.900	0.0052	3.9874(2)	9.111(1)
0.200	0.0059	3.8992(3)	7.532(2)	1.000	0.0000	**3.995(2)**	**9.151(5)**
0.300	0.0070	3.9023(3)	7.606(3)	**$BiOCl_{1-x}I_x$** (chlorine-rich phase)			
0.400	0.0077	3.9040(1)	7.683(1)	0.000	0.0000	**3.892(2)**	**7.375(2)**
0.500	0.0080	3.9083(2)	7.759(3)	0.002	0.0027	3.8926(2)	7.384(2)
0.600	0.0079	3.9133(3)	7.832(1)	0.005	0.0033	3.8914(4)	7.377(3)
0.700	0.0074	3.9153(3)	7.904(1)	0.100	0.0042	3.8914(2)	7.379(1)
0.800	0.0065	3.9185(2)	7.9747(8)	0.200	0.0057	3.8900(2)	7.376(2)
0.900	0.0052	3.9218(1)	8.0411(3)	0.400	0.0077	3.8910(5)	7.381(2)
1.000	0.0000	**3.9270(5)**	**8.106(1)**	**$BiOCl_{1-x}I_x$** (iodine-rich phase)			
$BiOBr_{1-x}I_x$				0.400	0.0077	3.9568(8)	9.03(1)
0.000	0.0000	**3.9270(5)**	**8.106(1)**	0.600	0.0081	3.958(1)	9.03(1)
0.100	0.0045	3.9311(2)	8.2682(9)	0.700	0.0076	3.9575(2)	9.040(5)
0.200	0.0060	3.9362(2)	8.4171(7)	0.760	0.0072	3.9604(2)	9.050(1)
0.300	0.0070	3.9424(3)	8.563(1)	0.820	0.0070	3.9696(5)	9.093(3)
0.400	0.0077	3.9478(2)	8.6860(8)	0.880	0.0059	3.9791(3)	9.121(1)
0.500	0.0080	3.9545(3)	8.800(2)	0.940	0.0050	3.9878(2)	9.140(1)
0.600	0.0079	3.9622(3)	8.903(2)	1.000	0.0000	**3.995(2)**	**9.151(5)**

Table 5. Lattice constants [Å] in the $BiOX_{1-x}Y_x$ systems.

[a] Numbers printed bold face refer to average values obtained from multiple measurements of the same compound.

small evacuated quartz ampoules to 550 °C for three days. Samples taken from the mixtures were then measured on a Stoe STADI-P powder diffractometer with NBS-Si as an external standard. All diffractograms of BiOCl–BiOBr and BiOBr–BiOI mixtures, as well as those of BiOCl–BiOI mixtures with $x < 0.02$ and $x > 0.74$, could be completely indexed and refined by assuming the presence of one tetragonal phase. Lattice constants were determined with the software WinXPow [25] and are given in Table 5. Selected mixtures were then mortared and heated for another 2 days to 550 °C. Lattice constants did not change significantly upon this procedure indicating that the reactions had been complete already after the first heating.

Error calculations

Often, when lattice constants are discussed as functions of x, no special attention is paid to the accuracy of the stated x values of the different mixtures investigated. However, in the above experiments, the x values have simply been calculated from the masses of the two components. This method of determining x certainly suffers from two sources of potential errors: weighing errors and impurities of the educts.

Effect of weighing errors: All BiOX–BiOY ["A/B"] mixtures were designed to amount to 100 ± 5 mg. The accuracy of the lab scale used, dm, is known to be about 0.3 mg. In assuming a linear error propagation (according to $|(\mathrm{d}x)_\mathrm{W}| = |(\partial x/\partial m_\mathrm{A})||\mathrm{d}m_\mathrm{A}| + |(\partial x/\partial m_\mathrm{B})||\mathrm{d}m_\mathrm{B}|$) the error in x, $(\mathrm{d}x)_\mathrm{W}$, can be calculated by

$$(\mathrm{d}x)_\mathrm{W} = (M_\mathrm{A}/M_\mathrm{B})[1+x(M_\mathrm{B}/M_\mathrm{A}-1)]^2\mathrm{d}m/(m_\mathrm{A}+m_\mathrm{B}) \quad (7)$$

with m_Q = mass, M_Q = molar mass of end member Q(Q = A,B), and $(m_\mathrm{A}+m_\mathrm{B})$ used as a constant. If $M_\mathrm{A} \approx M_\mathrm{B}$, eq. (10) simplifies to $(\mathrm{d}x)_\mathrm{W} \approx \mathrm{d}m/(m_\mathrm{A}+m_\mathrm{B})$, *i.e.*, $(\mathrm{d}x)_\mathrm{W} \approx 0.003$ for all $x(\neq 0,1)$ in the present case. For $x = 0$ and 1, weighing errors have no effect and $(\mathrm{d}x)_\mathrm{W} = 0$.

Effect of impurities: The purity of the BiOX compounds was initially checked by powder X-ray diffraction only. However, an impurity amounting to less than about 2% (molar) cannot be detected by this method. The error in x, $(\mathrm{d}x')_\mathrm{P}$, caused by such an impurity can be calculated using the modified linear error propagation relation $(\mathrm{d}x')_\mathrm{P} = (\partial x/\partial n_\mathrm{A})\mathrm{d}n_\mathrm{A} + (\partial x/\partial n_\mathrm{B})\mathrm{d}n_\mathrm{B}$($n_\mathrm{Q}$ = molar amount of end member Q) which has been formulated without using absolute quantities as dn_A and dn_B can never be greater than 0. We designate the molar fractions which consist of impurities in A and B as ε_A and ε_B, respectively (with ε_A, $\varepsilon_\mathrm{B} > 0$!). Then $\mathrm{d}n_\mathrm{A} = -\varepsilon_\mathrm{A}n_\mathrm{A}$ and $\mathrm{d}n_\mathrm{B} = -\varepsilon_\mathrm{B}n_\mathrm{B}$. Taking into account that $(n_\mathrm{A}n_\mathrm{B})/(n_\mathrm{A}+n_\mathrm{B})^2 = x - x^2$, we obtain

$$(\mathrm{d}x')_\mathrm{P} = (x-x^2)(\varepsilon_\mathrm{A}-\varepsilon_\mathrm{B}). \quad (8)$$

$|(\mathrm{d}x')_\mathrm{P}|$ is zero for $x = 0,1$; it reaches a maximum at $0.25(\varepsilon_\mathrm{A}-\varepsilon_\mathrm{B})$ for $x = 0.5$. Other than usual in error calculations, the positivity of ε_A and ε_B implies that $(\mathrm{d}x')_\mathrm{P}$ is a quantity for which the corresponding error bars point only to *one* side of the data points. The largest errors occur if only one component is contaminated. For example, if only A is contaminated by, say, 3%, then $(\mathrm{d}x)_\mathrm{max} = 0.25\varepsilon_\mathrm{A} = 0.0075$; if only B is contaminated by 3%, then $(\mathrm{d}x)_\mathrm{max} = -0.0075$. As in the present case any of the two end components could be pure and any of them could be contaminated (with $\varepsilon_\mathrm{A} = \varepsilon_\mathrm{B} = \varepsilon$), both signs have to be accounted for and we replace $(\mathrm{d}x')_\mathrm{P}$ by the quantity $(\mathrm{d}x)_\mathrm{P}$ (which now is supposed to cover *both* signs) according to

$$(\mathrm{d}x)_\mathrm{P} = (x-x^2)\varepsilon. \quad (9)$$

In Fig. 2, the horizontal widths of the data "points" symbolize errors $dx = (dx)_W + (dx)_P$, where the former have been calculated according to eq. (7), the latter according to eq. (9) by assuming $\varepsilon = 0.02$.

The results of the chemical analyses (see above) performed at a later stage as an additional check support the view that impurities in our educts are less than 2% or – at least – do not exceed 2% substantially.

Errors in lattice parameters: From the least-squares procedure in our indexing software the errors in *a* and *c* were in the ranges $(1-7)\cdot10^{-4}$ and $(0.5-5)\cdot10^{-3}$ Å, respectively (see Table 5). However, repeated measurements of some selected samples showed the errors rather to be $1\cdot10^{-3}$ for *a* and $5\cdot10^{-3}$ Å for *c*. These values were therefore uniformly taken for all data points with $x \neq 0,1$ in Fig. 2. For $x = 0$ and 1, the standard deviations obtained from the averaging of multiple measurements of the end members were used.

Errors in 2nd order function parameters: As usual in least-squares analyses, the standard deviations of A, B_1 and B_2 have been calculated by the visualizing software [26] from the deviations of the data points from the calculated function only. Uncertainties in data point positions have not been accounted for. To estimate the accuracy of the refined parameters as affected by the data point position errors, 2nd order functions have also been fitted to sets of data points at $x - dx, t + dt$ and others at $x + dx, t - dt$. Averaging the corresponding pairs of A, B_1 and B_2 resulted in practically the same parameter values as before, but in many cases in larger values for their standard deviations. In Table 4, the larger of the two values (the one derived conventionally and the one derived by the above procedure) is given; the former one is added as an alternative, but only in cases where it is smaller than the latter.

Acknowledgements

We are grateful to Mrs. Luitgard Rees-Isele for the preparation of the BiOX–BiOY mixtures and of the samples to be measured by powder diffractometry, furthermore to Mrs. Sigrid Hirth-Walter, Institut für Mineralogie, Petrographie und Geochemie der Universität Freiburg, for performing the chemical analyses.

[1] a) Phillips, Brandes Arch. **39**, 41 (1831); b) Muir, J. Chem. Soc. **29**, 145 (1876); **41**, 4 (1882); all references cited in Gmelins Handbuch der anorganischen Chemie, Vol. **19** (bismuth), Verlag Chemie, Berlin (1927).
[2] a) L. G. Sillén, Sven. Kem. Tidskr. **53**, 39 (1941); b) K. G. Keramidas, G. P. Voutsas, P. I. Rentzeperis, Z. Kristallogr. **205**, 35 (1993); c) J. Ketterer, V. Krämer, Acta Crystallogr. C**39**, 1098 (1986).
[3] a) du Pont de Nemours (R. D. Shannon), US Pat. 4252570 (February 24, 1981) [Chem. Abstr. **94**, 159116e (1981)]; b) Gebr. Cappelle Naamloze Vennootschap, Belg. (F. Vermoortele, E. J. Buyse), Eur. Pat. 1101801 (May 23, 2001) [Chem. Abstr. **134**, 368306a (2001)]; c) Ciba Speciality Chemicals Holding Inc. (M. Mueller, D. Bauer), Int. Pat. WO 2004099078 (Nov. 18, 2004) [Chem. Abstr. **141**, 425393 (2005)].
[4] A. F. Wells, Structural Chemistry, 5th ed., p. 1294, Clarendon Press, Oxford (1984).
[5] B. K. Vainshtein, V. M. Fridkin, V. L. Indenbom, Modern Crystallography, Vol. II, p. 116, Springer, Berlin – Heidelberg – New York (1982).
[6] R. D. Shannon, Acta Crystallogr. **A32**, 751 (1976).
[7] a) L. Vegard, Z. Phys. **5**, 17 (1921); b) L. Vegard, H. Dale, Z. Kristallogr. **67**, 148 (1928).
[8] a) A. V. G. Chizmeshya, M. R. Bauer, J. Kouvetakis, Chem. Mater. **15** , 2511 (2003); b) D. Zhou, B. F. Usher, J. Phys. D**34**, 1461 (2001).
[9] H. E. v. Steinwehr, Z. Kristallogr. **125**, 360 (1967).
[10] D. T. Hodul, J. M. Sienko, Inorg. Chem. **20**, 3655 (1981).
[11] V. S. Urusov, J. Solid State Chem. **98**, 223 (1992).
[12] A. R. Denton, N. W. Ashcroft, Phys. Rev. A**43**, 3161 (1991).
[13] C. Bocchi, S. Franchi, F. Germini, A. Baraldi, R. Magnanini, D. De Salvador, M. Berti, A. V. Drigo, J. Appl. Phys. **89**, 4676 (2001).
[14] a) E. T. Teatum, N. O. Smith, J. Phys. Chem. **61**, 697 (1957); b) Y. Rosenberg, V. Sh. Machavariani, A. Voronel, S. Garber, A. Rubshtein, A. I. Frenkel, E. A. Stern, J. Phys.: Cond. Matter **12**, 8081 (2000); c) S. Datta Roy (Paul), S. K. Das, Acta. Phys. Polon. **A97**, 671 (2000).
[15] W. E. Pearson, A Handbook of Lattice Spacings and Structures of Metals and Alloys, Vol. 1, Pergamon, New York (1967).
[16] a) M. Matsuura, S. H. Kim, M. Sakurai, K. Suzuki, Physica B**208**&**209**, 283 (1995); b) A. V. Andreev, L. Havela, V. Sechovsky, M. I. Bartashevich, J. Sebek, R. V. Dremov, I. K. Kozlovskaya, Phil. Mag. B**75**, 827 (1997); c) A. Nakatsuka, A. Yoshiasa, T. Yamanaka, Acta Crystallogr. B**55**, 266 (1999); d) T. Grygar, P. Bezdicka, J. Dedecek, E. Petrovsky, O. Schneeweiss, Ceram.-Silikaty **47**, 32 (2003).
[17] for example a) Yu. N. Grin, K. Hiebl, P. Rogl, H. Noel, J. Less-Comm. Met. **162**, 371 (1990); b) I. Kennedy, B. J. Kennedy, B. A. Hunter, T. Vogt, J. Solid State Chem. **131**, 317 (1997); c) D. De Salvador, M. Petrovich, M. Berti, F. Romanato, E. Napolitani, A. Drigo, Phys. Rev. B**61**, 13005 (2000).
[18] S. A. Hodorowicz, E. K. Hodorowicz, H. A. Eick, J. Solid State Chem. **50**, 180 (1983)

[19] a) J. E. Fischer, H. J. Kim, Phys. Rev. B**35**, 3295 (1987); b) S. Lee, H. Miyazaki, S. D. Mahanti, S. A. Solin, Phys. Rev. Lett. **62**, 3066 (1989).
[20] M. Weil, F. Kubel, Z. Anorg. Allg. Chem. **626**, 2481 (2000).
[21] T. Kusawake, Y. Takahashi, M. Y. Wey, K.-I. Ohshima, J. Phys.: Cond. Matter **13**, 9913 (2001)
[22] J. R. Dahn, W. R. McKinnon, R. R. Haering, W. J. L. Buyers, B. M. Powell, Can. J. Phys. **58**, 207 (1980).
[23] a) P. G. Bruce, M. Y. Saidi, J. Electroanalyt. Chem. Interfac. Electrochem. **322**, 93 (1992); b) D. G. Clerc, R. D. Poshusta, A. C. Hess, J. Phys. Chem. A**101**, 8926 (1997).
[24] SHELXTL, v. 6.14, Bruker AXS (2000).
[25] WinXPow, v. 1.09, the Stoe company, Darmstadt (2000).
[26] Origin, v. 7.0303, OriginLab Corporation, Northampton, MA (2002).